



HAL
open science

Chitin-Prussian blue sponges for Cs(I) recovery: From synthesis to application in the treatment of accidental dumping of metal-bearing solutions

C. Vincent, Y. Barre, Thierry Vincent, J. -M. Taulemesse, M. Robitzer, E. Guibal

► To cite this version:

C. Vincent, Y. Barre, Thierry Vincent, J. -M. Taulemesse, M. Robitzer, et al.. Chitin-Prussian blue sponges for Cs(I) recovery: From synthesis to application in the treatment of accidental dumping of metal-bearing solutions. *Journal of Hazardous Materials*, 2015, 287, pp.171-179. <10.1016/j.jhazmat.2015.01.041>. <hal-02914212>

HAL Id: hal-02914212

<https://hal.science/hal-02914212v1>

Submitted on 17 Feb 2025

HAL is a multi-disciplinary open access archive for the deposit and dissemination of scientific research documents, whether they are published or not. The documents may come from teaching and research institutions in France or abroad, or from public or private research centers.

L'archive ouverte pluridisciplinaire **HAL**, est destinée au dépôt et à la diffusion de documents scientifiques de niveau recherche, publiés ou non, émanant des établissements d'enseignement et de recherche français ou étrangers, des laboratoires publics ou privés.



HAL Authorization

Chitin-Prussian blue sponges for Cs(I) recovery: From synthesis to application in the treatment of accidental dumping of metal-bearing solutions

C. Vincent ^{a,b}, Y. Barré ^b, T. Vincent ^{a,1}, J.-M. Taulemesse ^c, M. Robitzer ^d, E. Guibal ^{a,*,1}

^a Ecole des mines d'Alès, Centre des Matériaux des Mines d'Alès, C2MA/MPA/BCI, 6 avenue de Clavières, F-30319 Alès Cedex, France

^b Commissariat à l'Energie Atomique, CEA Marcoule, DEN/DTCD/SPDE/LPSD, BP 17171, F-30207 Bagnols sur Cèze, France

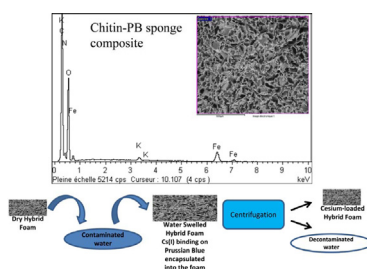
^c Ecole des mines d'Alès, Centre des Matériaux des Mines d'Alès, 6 avenue de Clavières, F-30319 Alès Cedex, France

^d Institut Charles Gerhardt – UMR5253, CNRS-UM2-ENSCM-UM1, ICGM-MACS-R2M2, 8 rue de l'Ecole Normale, F-34296 Montpellier Cedex 05, France

HIGHLIGHTS

- Prussian blue microparticles incorporated in chitin sponges.
- Efficient Cs(I) sorption after water absorption by dry hybrid sponge.
- Water draining after sorption for metal confinement and water decontamination.
- High decontamination factors and distribution coefficients for Cs(I) and ¹³⁷Cs(I).
- Effect of freezing conditions on porous structure and textural characterization.

GRAPHICAL ABSTRACT



ABSTRACT

Prussian blue (i.e., iron[III] hexacyanoferrate[II], PB) has been synthesized by reaction of iron(III) chloride with potassium hexacyanoferrate and further immobilized in chitosan sponge (cellulose fibers were added in some samples to evaluate their impact on mechanical resistance). The composite was finally re-acetylated to produce a chitin-PB sponge. Experimental conditions such as the freezing temperature, the content of PB, the concentration of the biopolymer and the presence of cellulose fibers have been varied in order to evaluate their effect on the porous structure of the sponge, its water absorption properties and finally its use for cesium(I) recovery. The concept developed with this system consists in the absorption of contaminated water by the composite sponge, the *in situ* binding of target metal on Prussian blue load and the centrifugation of the material to remove treated water from soaked sponge. This material is supposed to be useful for the fast treatment of accidental dumping of Cs-contaminated water.

Keywords:

Prussian blue
Chitin
Sponge
Cesium
Sorption
Water absorption
Structure-synthesis correlation

1. Introduction

Radioelements (including ¹³⁷Cs, which is a strong gamma emitter with high solubility and easy migration properties through groundwater to the biosphere, based on its chemical similarity

* Corresponding author. Tel.: +33 466782734; fax: +33 466782701.

E-mail address: Eric.Guibal@mines-ales.fr (E. Guibal).

¹ T.V. & E.G. are associated members of ICGM-MACS-R2M2.

to potassium) are generated along the conventional operation of nuclear power plants and the treatment of the effluents generated in the processing of spent nuclear fuels is a critical step in the management of nuclear facilities. Apart these conventional and well-controlled effluents, accidents such as the Fukushima disaster in 2011 are generating hazardous sources of radioelement-bearing solutions. The development of treatment processes for the fast and efficient recovery of radioelements, even in complex media (such as sea water), is thus a priority for reinforcing the safety of the entire nuclear industry. In the case of conventional controlled effluents several processes exist using ion-exchangers (such as Prussian blue, PB), titanate-based materials or clays and mineral oxides. In the case of accidental dumping of small amounts of contaminated effluents there is a need for developing alternative processes capable of simultaneously recovering and treating the contaminated water. This is the objective of the present work: associating (a) a sponge, which is targeted to absorb water, and (b) an ion-changer tailored for binding the radioelement. The elimination of water by centrifugation in the next step, allows releasing decontaminated water while the radioelement is concentrated on the hybrid solid phase.

Prussian blue (PB) is an ion-exchanger (IE) that is well known for its affinity for some light earth metal ions such as cesium(I) or rubidium(I) but also for thallium(I) [1]. This is part of the conventional treatment of acute poisoning with radioactive Cs (Radiogardase®) [2]. For medical applications, Prussian blue is conditioned under the form of tablets/capsules to be ingested; cesium binding to insoluble PB occurs in the gastro-intestinal tract before being excreted from natural ways. Prussian blue is generally synthesized by reaction of potassium (or sodium) hexacyanoferrate with iron(III) chloride giving different compounds with different solubility properties. In the presence of an excess of iron(III) chloride, PB turns from a soluble/colloidal form ($KFe[Fe(CN)_6]$) to an insoluble form generally described as $Fe_4[Fe(CN)_6]_3$. Cesium(I) is then exchanged with K or Fe present on the lattice of the IE (cubic lattice structure) [1]. Actually, the composition and properties of these PB-based compounds are strongly influenced by the experimental conditions used for PB synthesis, such as molar ratio between the precursors, the order of addition and mode of agitation: the proportion of K and Fe exchangeable moieties may strongly change and the solubility of the final product as well. Several studies on PB analog (other metal-potassium hexacyanoferrate compounds) have clearly shown the importance of these operating parameters on the properties of final products [3–5]. The presence of colloidal species makes difficult the recovery of the IE at the end of the synthesis procedure and in some cases the addition of a coagulant/flocculant (such as chitosan) was reported to contribute to (a) charge neutralization, and (b) agglomeration for ready recovery and further inclusion in biopolymer matrix [6].

In any cases the small size of these IE particles makes their use complex at large scale due to difficulty in recovery (coagulation/flocculation, settling etc.); and it is generally helpful immobilizing the IE in a suitable matrix (biopolymer, polymer) or at the surface of a specific mineral support (silica, activated carbon, zeolite etc.) [7–13]. These methods lead to materials that can be used in tank reactor, fixed-bed columns for the treatment of controlled contaminated water streams. Biopolymers such as alginate and chitosan have been recently reported as potential encapsulating materials for the immobilizations of IEs, including double metal hexacyanoferrate [8,14–17]. The physical versatility of the biopolymers allows developing different shaping and conditioning of these materials such as beads [11,15], membranes, fibers [18], or tubes [19], but also very highly porous foams [20–22]. The present study combines the incorporation properties of chitosan for PB with a specific conditioning of the biopolymer under the form of highly porous sponges. In order to improve the chemical

resistance of the material with changing operational conditions (pH changes, especially), the composites are finally reacylated for producing chitin-PB sponges [23,24]. Cellulose fibers are introduced in the composite to reinforce the mechanical stability of the material [25,26]. The objective is to design a sponge that could be used for the treatment of contaminated water in the case of accidental dumping. After the absorption of metal-containing water on the composite sponge, the IE (i.e., PB) rapidly binds Cs(I) ions through ion-exchange mechanism (more generally adsorption). After water wringing (or centrifugation) from wetted sponge, decontaminated water can be environmentally friendly rejected to water discharge network while the metal is confined in the composite sponge. In order to reach this objective the present study (a) synthesizes a series of composite materials (containing chitosan (further reacylated to chitin), Prussian blue (BP) particles and cellulose fibers (which may contribute to improve the mechanical resistance of the foams) and (b) compares their structural and textural properties; their ability to absorb water and finally to bind Cs(I) (both in natural and nuclide forms; i.e., ^{133}Cs and ^{137}Cs , respectively).

2. Material and methods

2.1. Materials

Potassium hexacyanoferrate ($K_4[Fe(CN)_6] \cdot 3H_2O$, Riedel-de Haën), iron(III) chloride ($FeCl_3 \cdot 3H_2O$, Chem-Lab), acetic anhydride ($C_4H_6O_3$, Sigma-Aldrich) were supplied as reagent grade products. Acetic acid (80% w/w, Carlo Erba), ethanol (96% w/w, Sodipro) were technical products. Chitosan (molecular weight 125,000 $g \cdot mol^{-1}$, deacetylation degree: 87%) was supplied by Aber-Technologies (France). Cesium nitrate was purchased from Merck AG (Germany). Cellulose fibers were prepared from an Ahlstrom raw paper substrate (Pont-Evêque, France) by dilacerations and rehydration. This is a Roburflash-type paste prepared from resinous wood (long fibers) and with poor refinery level (flash).

2.2. Synthesis of composite sponge

The elaboration of composite materials followed basically five main phases: (a) the synthesis of PB, (b) the stabilization of the complex with chitosan, (c) the shaping (and freeze-drying) of chitosan-PB sponges, (d) the freeze-drying of the sponge, and (e) the reacylation of chitosan to prepare chitin-PB sponge.

The synthesis of PB complex consisted in the mixing of two precursors for 30 min under strong agitation: (i) potassium hexacyanoferrate (100 mL, 3.62 g), and (ii) iron(III) chloride was used (100 mL, 2.23 g). The molar ratio between iron(III) and potassium hexacyanoferrate was set at 1.2:1. The hexacyanoferrate solution was injected in the metal precursor solution drop-by-drop. At the end of this first step, 1 L of demineralized water was added to the suspension. This suspension was then added to 2 L of chitosan solution (at 0.05%, w/w) to stabilize the complex (charge neutralization, partial or complete) and improve the settling of the material that can be readily recovered by filtration on paper membrane. This wet material (chitosan-stabilized complex, CSC) was thus mixed with 100 mL of water and 100 mL of a 4% w/w chitosan solution in two steps: softly, and then under UltraTurax (24,000 rotations min^{-1} , for 5 min). This last step was also performed changing the concentration of chitosan solution to 6% w/w to prepare two different compounds with final chitosan concentrations of 2% and 3% w/w, respectively. In order to verify the impact of PB load in the material the amount of IE was divided by 2 or by 3 to prepare the corresponding lots. The last parameter that was varied was the presence of cellulose fibers added at the level of 1% w/w in the final suspension.

The shaping of the material was performed by dropping the viscous chitosan/stabilized complex suspension into plane rectangular molds that were frozen at different temperatures: -20°C , -80°C or immersed in liquid nitrogen (i.e., -196°C). The change in freezing temperature may affect the freezing ramp, the crystallization speed of water in the mixture and finally the macroporous properties of the materials [21,27]. After the freezing step, the materials were rapidly recovered from the molds and freeze-dried overnight.

The final step consisted in the re-acetylation of chitosan [23,24]. One gram of chitosan-PB composite was mixed with 40 mL of ethanol and 10 mL of acetic anhydride under reflux for 1 h. The products were then rinsed once with ethanol to remove non-reacted reagent and finally rinsed three times with demineralized water. The chitin-PB sponges were finally freeze-dried.

2.3. Characterization of composite sponge

2.3.1. SEM & SEM-EDX analysis & simplified mechanical tests

The morphology and the distribution of inorganic ion-exchanger (and Cs element, when relevant) in the materials were determined with a scanning electron microscope coupled with energy dispersive X-ray analysis (SEM-EDX). SEM observations were performed using an environmental scanning electron microscope (ESEM) Quanta FEG 200, equipped with an OXFORD Inca 350 energy dispersive X-ray microanalysis (EDX) system. The use of environmental SEM allowed the direct observation of materials, without previous metallization of the samples. The topography of the samples was observed using secondary electron flux while the backscattered electrons were used for the identification and localization of heavy metals at the surface of the materials (by phase contrast). SEM-EDX facilities were used for the detection of elements and their semi-quantitative analysis (Cs and principal elements representative of the inorganic ion-exchanger; i.e., Fe, K elements). The standard accelerating voltage was set at 15.0 keV. The samples were analyzed on freshly cut sections (mechanical after liquid nitrogen "icing").

Mechanical tests (Stress-Strain) were performed using the facilities of the SEM equipped with a mechanical testing unit (Benco symmetrical bench) on the sponges (5×40 mm). The sponges, fixed inside the SEM by jaws, were submitted to a stress test, after an axial cut (length: 1 mm) was operated on each side of the sponge to orientate the deformation of the material in the specific analytical area. The SEM facilities allow to follow the force measured on the sensors and the elongation of the sponge submitted to a 5 kN stress strength. A video reporting a series of microphotograph of the stretching area could be recorded for each sample. Elastic, plastic and striction/rupture areas have been identified on the strength vs. elongation curves, and used to calculate the mechanical constants: Young modulus, E ; resistance to stress, R_m ; and elongation at the rupture A_r (see Additional Material Section). Since the tests are not normalized the results will be considered as indicative and will only be used for the comparison of the different sponges.

2.3.2. Water absorption

The water absorption was determined through 2 procedures. Initially, a given amount of dry sponge (m_{dry}) was soaked in demineralized water (m_{soaked}). In the first procedure, free water (only absorbed in the porous structure of the sponge) was dripped and the wet sponge was weighted (m_{dripped}) and compared with dry mass to evaluate the water that was bound to the sponge; i.e., a first value of the water absorption capacity.

In the second procedure, the soaked sponge (which was initially dripped) was centrifuged in a centrifugal tube (where a grid served to separate the solid from the liquid phase) ($m_{\text{centrifuged}}$) and the amounts of water bound to the sponge and absorbed in

the porous network were systematically quantified. These values served to evaluate the water absorption capacity (mL g^{-1}). These water absorption values were determined for different compositions of chitin-PB sponges.

2.4. Cs(I) sorption tests

A given amount of dry sponge (m_{dry}) was added to a given amount of water containing fixed concentrations of Cs(I) (C_0 , mg Cs L^{-1}). The amount of solution (V , L) in contact with the sponge was set a little higher than the corresponding water absorption values. The sponge was simply used in a static mode. After fixed contact time the soaked sponge was centrifuged and the residual concentration of Cs(I) (C_{eq} , mg Cs L^{-1}), was measured by atomic absorption spectrometry (AAS, Varian AA20 spectrometer; wavelength, λ : 852.1 nm). Mass balance was used to quantify the sorption capacity (q , Cs(I) concentration in the sponge):

$$q = \frac{V \times (C_0 - C_{\text{eq}})}{m_{\text{dry}}}$$

The distribution coefficient, K_d (L kg^{-1}), was obtained by:

$$K_d = \frac{q}{C_{\text{eq}}}$$

The tests on $^{137}\text{Cs(I)}$ sorption have been operated using the same procedure (adjusting the volume of solution to the amount of sponge, based on its water absorption capacity). Typically, 1 mL of $^{137}\text{Cs(I)}$ spiked solution was put in contact with a piece of sponge (about 75 mg) for 1 min or for 3 min. The wet sponge was transferred to a centrifugation tube filled with glass beads. After centrifugation the sponge was removed and the tube was rinsed with 50 mL of demineralized water. Fifty mL were dropped in the analytical flask for gamma counting (using a Eurisy Mesures counter equipped with a germanium detector). The activity of the initial solution (A_0 , Bq L^{-1}) was measured at 37000 Bq L^{-1} . The residual activity (A_r , Bq L^{-1}) was measured and used to calculate the decontamination factor (DF: A_0/A_r) and the distribution coefficient (K_d^{137} , L g^{-1} : $\text{Cs}_{\text{sorbent}}/\text{Cs}_{\text{solution}} = (A_0 - A_r)V/(mA_r)$). Another experiment was performed using a Cs(I) (0.13 mg L^{-1}) + $^{137}\text{Cs(I)}$ solution to work at higher level of cesium. Postulating that Cs(I) and $^{137}\text{Cs(I)}$ are equally adsorbable, it was possible evaluating the total sorption capacity by measurement of the residual activity of $^{137}\text{Cs(I)}$.

3. Results and discussion

3.1. Composite sponge characterization

3.1.1. Structure

The structure of the sponges was characterized by SEM analysis for different operating conditions in order to evaluate the relative effect of freezing temperature and biopolymer concentration. The observed structures are quite similar to those obtained by Madhally and Matthew [20]. Fig. 1 shows the topographic observation of the different materials at a large scale (magnification $\times 50$) in order to evaluate their homogeneity. Previous studies reported the strong influence of cooling conditions (temperature, temperature ramp) on the organization of the porous scaffold on several biopolymers [20,27]. When the freezing of the biopolymer-PB solution occurs at -20°C the sponge is characterized by heterogeneous and not organized structures, regardless of the concentration of the biopolymer in the encapsulation mixture. In comparison, the sponges prepared at -80°C and in liquid nitrogen (i.e., -196°C) appear to be more homogeneous and have a dense structure. The aspect of the sponges frozen in liquid nitrogen seems to be independent of the concentration of the biopolymer. When running

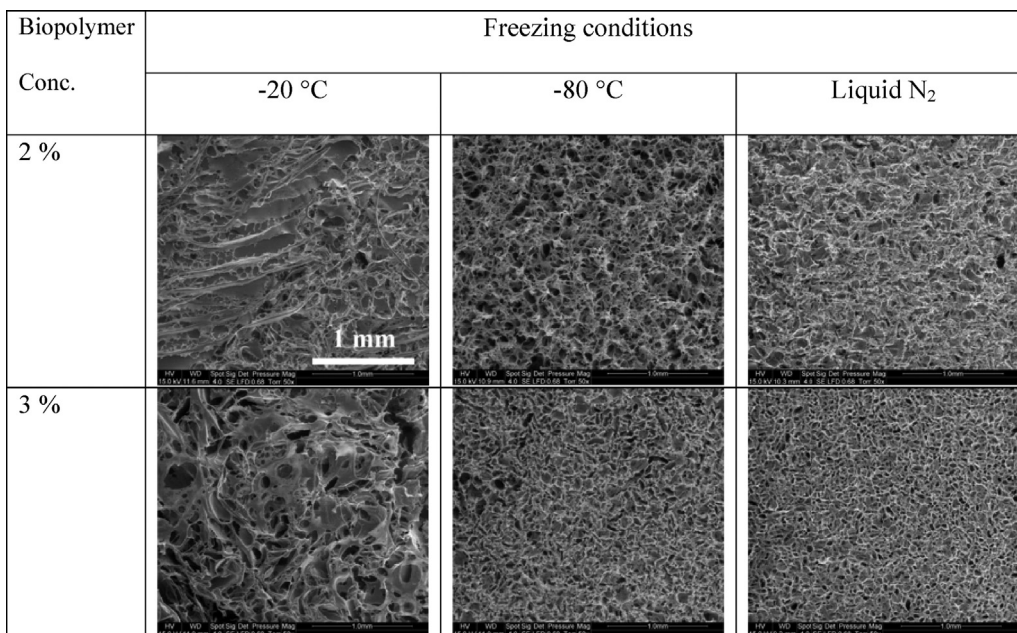


Fig. 1. Influence of synthesis parameters on the structure of composite chitin/PB sponges (SEM analysis; Secondary electrons detection; Magnification: $\times 50$, the bar represents 1 mm).

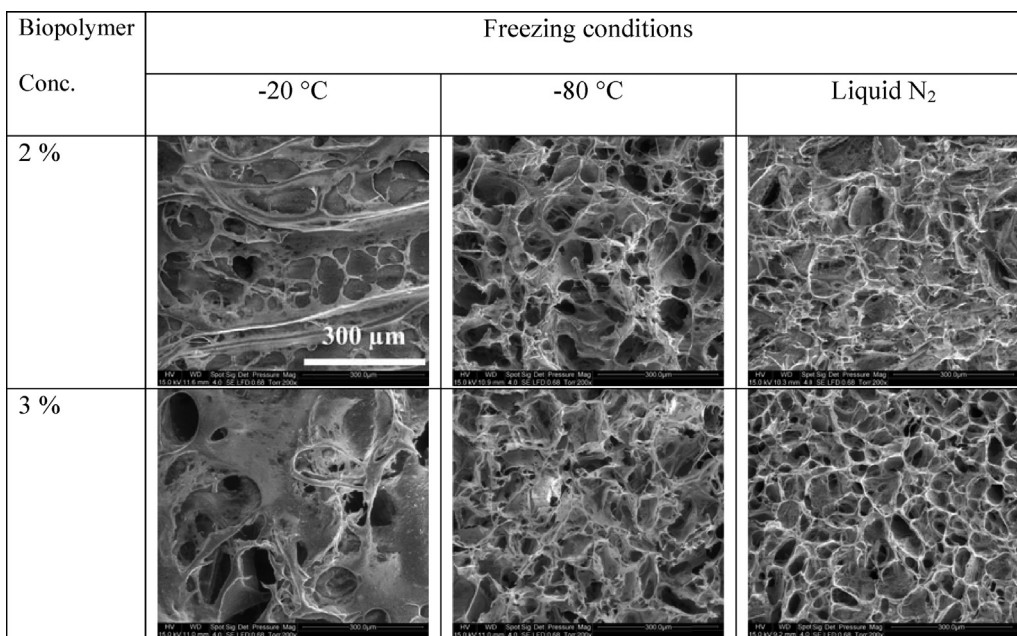


Fig. 2. Influence of synthesis parameters on the structure of composite chitin/PB sponges (SEM analysis; Secondary electrons detection; Magnification: $\times 200$, the bar represents 300 μm).

the freezing of the sponge at -80°C the response is intermediary: with 2% and 3% w/w biopolymer concentrations the materials are homogeneous but at low biopolymer concentration the sponge network shows a slightly more opened structure than at higher biopolymer concentration. These conclusions are confirmed by the comparison of the microphotographs at higher magnification (i.e., $\times 200$) (Fig. 2). It is noteworthy that at higher biopolymer concentration the “opening of the porous cells” seems to be little reduced compared to those obtained with 2% w/w chitosan solutions. At low freezing temperature (-20°C) the porosity appears different, showing larger holes but globally much larger plane foils. Increasing more the magnification (up to $\times 2000$) allows observing the

surface of planar structures that constitute the architecture of the porous network (Fig. 3). These surfaces are characterized by granular structures that probably represent the inorganic ion-exchanger micro- or nano-particles partially agglomerated after addition of chitosan at the coagulation/flocculation stage of the synthesis procedure.

layer around the cellulose fibers.

BET analysis on similar biopolymer-based foams using uncontrolled drying procedures (freeze-drying at -53°C is not sufficient to prevent the collapse of the microporous structure of the biopolymer) showed very low values (i.e., a few $\text{m}^2 \text{g}^{-1}$) (personal unpublished data). The differences between the different materials

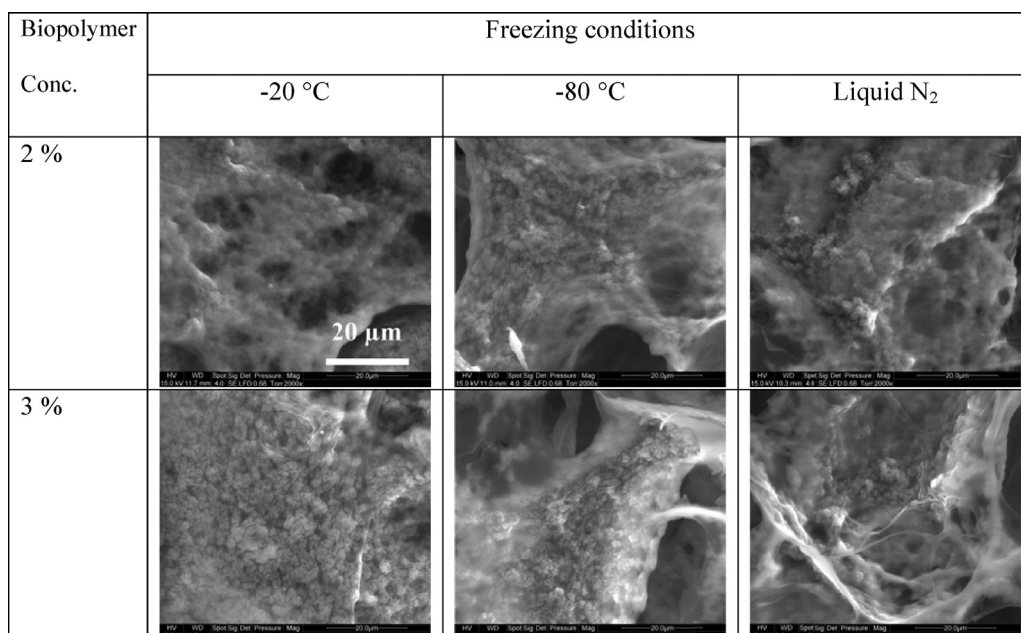


Fig. 3. Influence of synthesis parameters on the structure of composite chitin/PB sponges (SEM analysis; Secondary electrons detection; Magnification: $\times 2000$, the bar represents $20\ \mu\text{m}$).

(characterized by a very high macro-porosity) are not expected to be significant. A significant improvement in the interfacial properties of these materials would consist in simultaneously managing the macro-porosity of the foam and the microporous structure of biopolymer gels. This is currently under consideration in our research groups.

The effect of temperature is directly correlated to the kinetics of freezing; this controls the rearrangement of water inside the material. With very low temperature the freezing is fast (at $-80\ ^\circ\text{C}$) and even instantaneous (in nitrogen liquid, at $-196\ ^\circ\text{C}$), while at $-20\ ^\circ\text{C}$ the icing of water takes enough time to let water packs rearrange to form large, heterogeneous channels. Yuan et al. [27] reported that fast cooling induced non-simultaneous nucleation and generated

directional pore structures while simultaneous nucleation and uniform and isotropic structures were obtained with the slow cooling ramp. These conclusions are not fully consistent with the present results: the freezing at $-20\ ^\circ\text{C}$ results in slower cooling process compared to the other temperatures and the materials prepared under these conditions were less homogeneous. However, the fast freezing that occurs at $-80\ ^\circ\text{C}$ and in liquid nitrogen resulted in more-oriented porous network. While increasing the concentration of the biopolymer the movement of water bodies is affected leading to some changes in the porous structure of the sponges. Madihally and Matthew reported that increasing the concentration of chitosan decreased the size of the pores, independently of the freezing temperature [20]. The size and the organization of the

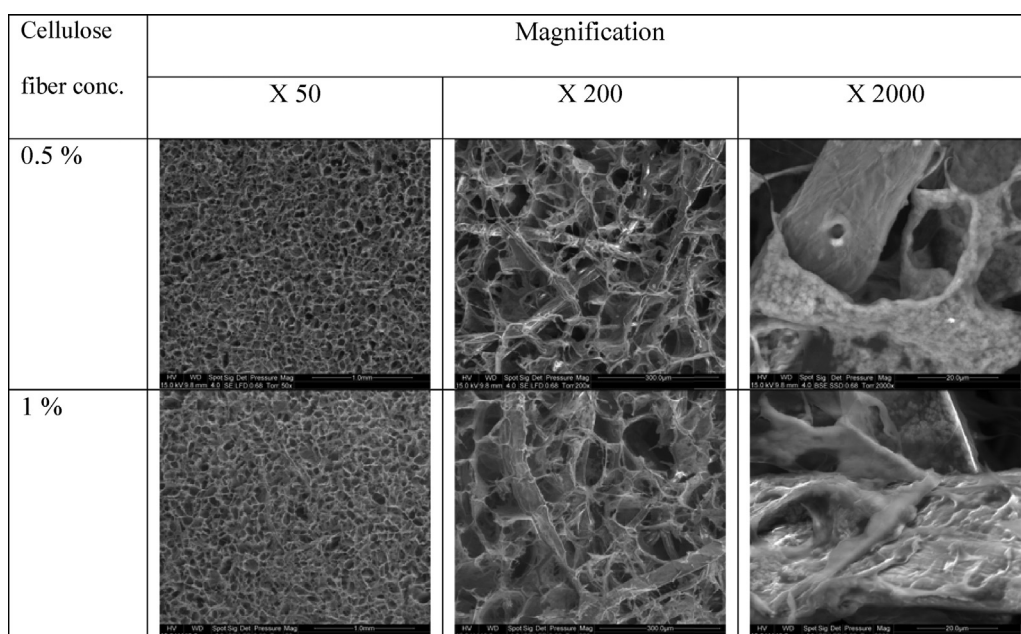


Fig. 4. SEM analysis of chitin-PB composite sponges with inclusion of cellulose fibers (at different loads, 0.5% and 1% of the solution mixture) at different magnifications (Secondary electrons detection).

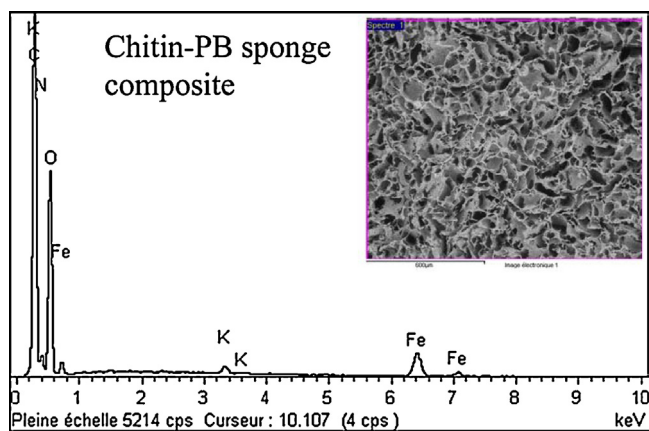


Fig. 5. SEM-EDX analysis of a chitin-PB sponge composite (freezing temperature: -80°C for shape-forming; biopolymer concentration: 3% w/w).

Table 1

Element analysis (by SEM-EDX analysis; accelerating voltage: 15 kV) of a chitin-PB sponge composite (freezing temperature: -80°C ; biopolymer concentration: 3% w/w).

Element	Weight fraction (%)	Weight fraction σ (%)	Atomic fraction (%)
C	46.7	0.5	56.2
N	10.0	0.7	10.3
O	34.4	0.4	31.1
K	0.5	0.05	0.2
Fe	8.4	0.2	2.2

porous structure (orientation of pores) depend also on the temperature ramp (freezing rate) and the density of the material.

The introduction of 0.5% or 1% w/w of cellulose fibers (reported herein for the $-80^{\circ}\text{C}/3\%$ w/w synthesis conditions) is shown on Fig. 4. At low magnification (i.e., $\times 50$) the materials are homogeneous and the cellulose fibers are difficult to identify. When increasing the magnification to $\times 200$ and to $\times 2000$, the strips of cellulose fibers embedded with chitosan are clearly appearing in the frame of the porous network. In the sponges the cellulose fibers play the role of armatures that contribute to reinforce their mechanical properties. The micro- or aggregated nanoparticles of PB appear at the highest magnification in the embedment chitin/chitosan

Fig. 5 shows the SEM-EDX analysis of the chitin-PB sponge (produced by freezing at -80°C with 3% w/w biopolymer solution). Main elements are O (tracer of encapsulating material), C and N (associated to both the encapsulating material and PB), and K and Fe (specific to PB). The presence of K element indicates that the ion-exchanger immobilized in the sponge is not “pure” insoluble PB but may also contain partially soluble (colloidal) forms of PB, which were collected through the coagulation-flocculation of these colloids using chitosan in the synthesis procedure. Table 1 reports the elemental analysis obtained from SEM-EDX analysis. The fraction of K element is substantially lower than that of Fe; this means that the fraction of soluble PB remains negligible (about 10%) compared to the insoluble fraction.

3.1.2. Water absorption

Swelling and water absorption increase when decreasing the degree of deacetylation. This is correlated to the increase of the d-space in the crystalline structure of the biopolymer when the deacetylation degree decreases [28]. In the present study chitosan was reacylated; this contributes to increase water absorption capacity of chitin-based materials. The water absorption properties depend on the composition of the sponges (presence of cellulose fibers, presence of PB) as shown in Table 2. Experimental condi-

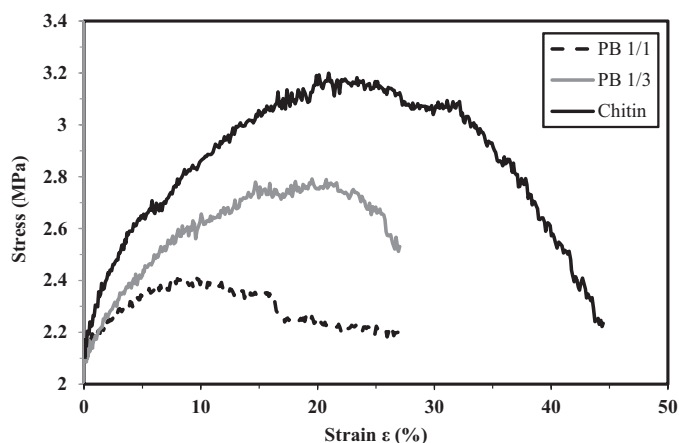


Fig. 6. Mechanical testing (stretching test) of chitin-PB sponge composite (and reference chitin sponge) using SEM-mechanical testing unit. Approach of strength-elongation curves (applied strength: 5 kN; dimensions of the sponge: 5×40 mm; the sponges were systematically prepared with 1% (w/w) load of cellulose fibers).

tions for the synthesis of the sponge were selected on the basis of SEM observations: freezing temperature set at -80°C , and 3% w/w biopolymer concentration. Indeed, Hsieh et al. [21] reported that water absorption reduces with the decrease in the size of the pores. SEM microphotographs (Figs. 1 and 2) showed that the freezing in liquid nitrogen gave smaller pore sizes than the -80°C process. This freezing temperature was preferred for the better homogeneity of the sponges.

reports the results obtained. Water absorption ranged between 13.1 and 13.7 mL g^{-1} , while the amount of water retained varied in the range 1.7–2.0 mL g^{-1} consistently with previous results. Even with Cs(I) concentrations as high as 356 mg Cs L^{-1} (for an amount of sponge close to 70 mg and a volume of solution close to 1 mL) the retention yield remained higher than 99.8% with a distribution coefficient, K_d , up to 17,300 L kg^{-1} . The residual concentration remained below 0.3 mg Cs L^{-1} . As expected, increasing the amount of metal increases the sorption capacity; however, the objective of the composite chitin-PB sponge being the full recovery of the metal (potentially radioelement) it is mandatory to completely eliminate the metal in the water discharged from centrifuged sponge. Tests with $^{137}\text{Cs(I)}$ solutions with very low levels of detection bring supplementary information on the potential of the sponges to recover metal traces.

3.2.3. $^{137}\text{Cs(I)}$ sorption preliminary test

The tests performed on $^{137}\text{Cs(I)}$ solutions and Cs(I) (0.13 mg Cs L^{-1}) solutions spiked with $^{137}\text{Cs(I)}$ are reported on Table 6

First, the materials exhibit substantial capacities for water absorption: the water absorption ranged between 14 and 18 mL g^{-1} (d.w.). Surprisingly, highest levels were obtained with chitin sponges (without cellulose fibers and PB). The addition of 1% (w/w)

Table 2

Water absorption for different chitin-PB sponge composites—effect of cellulose fibers, and PB relative concentration.

Sample	Chitin (%)	PB (%)	Cell Fibers (%)	Water absorption (mL g^{-1})
Chitin	100	—	—	17.7
Chitin + 1% Cell. Fib.	67	—	33	16.0
Chitin + PB	84	16	—	14.3
Chitin + PB + 1% Cell. Fib.	56	16	28	15.7
Chitin + PB (1/2) + 1% Cell. Fib.	61	8	31	16.3
Chitin + PB (1/3) + 1% Cell. Fib.	63	5	32	16.0

Synthesis procedure: freezing temperature -80°C ; biopolymer concentration 3% w/w.

Table 3
Mechanical properties–stretching tests.

Sample	Young modulus, E (MPa)	Resistance to stretching R_m (MPa)	Relative elongation at rupture, A_r (%)
Chitin	0.50	3.2	28
Chitin-PB 1/1	0.23	2.4	14
Chitin-PB 1/3	0.20	2.8	22

Table 4
Sorption tests–Uptake kinetics (C_0 : 93.6 mg Cs L⁻¹).

Contact time(s)	Dry mass (mg)	Wet mass (g)	Absorbed water (mL g ⁻¹)	Retained water ^a (mL g ⁻¹)	C_t (mgCs L ⁻¹)	Cs retention yield (%)	K_d^b (L kg ⁻¹)
30	66.3	1.048	14.81	1.71	1.82	98.1	747
60	81.8	1.079	12.20	2.05	0.1	99.9	11,404
300	79.0	1.076	12.62	1.91	<0.01	≈100	>11,000

^a Mass balance on water after centrifugation of wet sponge.

^b K_d calculated on the basis of initial and final concentration of Cs(I) in the impregnating solution and in the centrifuged phase, and the dry mass of chitin-PB sponge composite:

$$K_d = \frac{(\text{Wet mass} - \text{Dry mass}) \times (C_0 - C_t)}{\text{Dry mass} \times C_t}$$

Table 5
Sorption tests–effect of initial Cs(I) concentration on treatment efficiency (at equilibrium).

C_0 (mgCs L ⁻¹)	Dry mass (mg)	Wet mass (g)	Absorbed water (mL g ⁻¹)	Retained water ^a (mL g ⁻¹)	C_{eq} (mgCs L ⁻¹)	Cs retention yield (%)	K_d^b
93.6	74.2	1.079	13.54	1.94	< 0.01	≈100	>11,000
218	73.9	1.043	13.12	1.76	0.23	>99.8	12,418
356	70.2	1.027	13.63	1.78	0.28	>99.9	17,327

^a mass balance on water after centrifugation of wet sponge. ^b K_d calculated on the basis of initial and equilibrium concentration of Cs(I) in the impregnating solution, and in the centrifuged phase, and the dry mass of chitin-PB sponge composite:

$$K_d = \frac{(\text{Wet mass} - \text{Dry mass}) \times (C_0 - C_{eq})}{\text{Dry mass} \times C_{eq}} \text{ (dimensionless)}$$

of cellulose fibers in the preparation lead to a substantial decrease in water absorption (from 17.7 to 16 mL g⁻¹). On the other hand the addition of PB to chitin had a more marked impact on water absorption (from 17.7 to 14.3 mL g⁻¹). However, the introduction of cellulose fibers partially restored the ability of the sponge to absorb water (close to 15.7 mL g⁻¹). It is noteworthy that with the presence of cellulose fibers the water absorption capacity of the composite sponges was not significantly affected by the amount of PB incorporated (16 ± 0.3 mL g⁻¹). From these results it appears that the incorporation of cellulose fibers or PB slightly decreases the ability of chitin sponge to absorb water and that the presence of cellulose fibers tends to decrease the impact of PB incorporation on water absorption capacity.

These results are also important for evaluating the amount of water that can be treated with a given amount of dry sponge. These values have been used for selecting experimental conditions for Cs(I) sorption experiments.

3.1.3. Effect of Prussian blue on mechanical properties of chitin-PB sponges

The testing of mechanical properties has been operated using the facilities of the mechanic testing unit of the SEM system. These are not standardized/normalized tests but the qualitative comparison of the Stress–Strain curves for the different systems is indicative of their relative mechanical stretching properties (Fig. 6). Obviously, the introduction of PB in the chitin sponge significantly influences the resistance of the composite material to stretching: both the maximum strength and the elongation profiles were negatively impacted. It is noteworthy that when the amount of PB entrapped in the sponge decreases the mechanical properties are improved. Table 3 reports the main mechanical characteristics of the sponges (to be considered only for comparison). The introduc-

tion of PB particles decreased the Young modulus, the resistance to stretching and the elongation properties, and this decrease tended to be less marked when the PB was “diluted” in concentration in the sponge. The presence of micro- or nano-particles contributes to reduce the cohesion of the composite material, despite the positive effect of cellulose fibers. Suwanchawalit et al. [29] compared the mechanical properties of different composites based on macroporous chitosan scaffolds and TiO₂ particles. The size of mineral particles (6–200 nm) and the characteristics of their incorporation (in the core of the foam structure vs. partial embedment) are critical parameters for the mechanical properties of the composite sponge.

3.2. Cs(I) sorption tests

These tests are based on a concept quite different to conventional sorption systems. Indeed, the objective is to design a sponge to recover Cs(I) from accidental dumping like for domestic cleaning systems, and not to really evaluate maximum sorption capacities. So, the experimental conditions, especially the contact between fixed volume of solution and appropriate amount of dry sponge, are determined in function of the water absorption capacity of the sponges, taking into account the sponge dewatering by centrifugation. The final objective is to design experimental conditions, both in terms of equilibrium and kinetics for full decontamination of dumped water with complete transfer of the metal into the centrifuged sponge.

3.2.1. Kinetic test

The kinetics tests are reported in Table 4. The absorbed water ranged between 12.2 and 14.8 mL g⁻¹ and the retained water corresponded to values between 1.7 and 2.1 mL g⁻¹. The retention yield is quite high (>98%) due to the large excess of ion-exchanger

Table 6
Sorption tests on $^{137}\text{Cs(I)}$ solutions (and composite $\text{Cs(I)} + ^{137}\text{Cs(I)}$ solutions).

A_0 (Bq L $^{-1}$)	C_0 (mg Cs L $^{-1}$)	Time (min)	A_r (Bq L $^{-1}$)	C_r ($\mu\text{g Cs L}^{-1}$)	Cs retention yield (%)	K_d^{137}
37,000	0	1	1650	–	95.5	300
37,000	0	3	<6	–	>99.98	>88,000
37,000	0.13	1	1150	6.0	96.9	440
37,000	0.13	3	<6	2×10^{-2}	>99.98	>88,000

A_0/A_r and C_0/C_r : initial/residual $^{137}\text{Cs(I)}$ activities and Cs(I) concentrations.

$$K_d^{137} = \frac{(\text{Wet mass} - \text{Dry mass}) \times (A_0 - A_r)}{\text{Dry mass} \times A_r} \text{ or } K_d^{137} = \frac{(\text{Dry mass} - \text{Wet mass}) \times (C_0 - C_r)}{\text{Dry mass} \times C_r}$$

in the composite chitin-PB sponge compared to Cs(I) amounts. With a contact time of 1 min the retention of Cs(I) yielded up to 99.9%; this corresponds to a distribution coefficient K_d higher than $11,000 \text{ L} \cdot \text{kg}^{-1}$. When increasing the contact time to 5 min, the recovery of the metal can be considered as complete (below the detection limits of the analytical procedure). These preliminary results confirm the fast binding of Cs(I) through the selected experimental procedure.

3.2.2. Sorption performance–effect of initial metal concentration

The same experiment was performed with increasing concentrations of Cs(I) in the dumped water (in the range $94\text{--}356 \text{ mg Cs L}^{-1}$) and the contact time was set to 3 h (large excess compared to required time on the basis of kinetic results) before centrifugation. Table 5, using an experimental procedure derived from the procedure that was followed in the preceding section: solution absorption, swelled sponge centrifugation and ^{137}Cs counting on centrifuged solution. These results confirm the efficiency of the composite sponges for the absorption and the treatment of radionuclide-bearing solutions: after 1-min contact time the residual concentration (or activity) of the solution was reduced by 95–97%, and the distribution coefficient varied between 300 and 440 L g^{-1} . When increasing the contact time to 3 min, the Cs(I) recovery yields increased above 99.98% and the distribution coefficient exceeded 88000 L g^{-1} . Actually the residual activity after 3 min of contact was systematically below the detection limit (i.e., 6 Bq L^{-1}).

4. Conclusion

The encapsulation of synthesized Prussian blue in chitosan sponge (followed by biopolymer reacetylation) allowed preparing an efficient material for the absorption of contaminated water combined with the transfer of the contaminant from the aqueous solution to the immobilized ion-exchanger. Several operating parameters have been tested for the optimization of sponge manufacturing: SEM analysis helped in evaluating the contribution of these experimental parameters on the morphological characteristics of the sponges. The best biopolymer concentration for PB encapsulation was found to be around 3% (w/w). The conditioning of the material includes a freezing step in the synthesis procedure and the best temperature was found to be close to -80°C . The presence of cellulose fibers improves the mechanical resistance to stretching of the sponges and partially compensates the negative effect of the incorporation of micro- and nano-particles of PB. Water absorption ranges around $12\text{--}14 \text{ mL g}^{-1}$ depending on experimental conditions, with retention of water (after centrifugation) in the range of $1.7\text{--}2.0 \text{ mL g}^{-1}$. This means that the dry sponges can be used to treat about $10\text{--}12 \text{ mL}$ of water per g of sponge. The retention of Cs(I) exceeds 99% in the wide range of metal concentration (under conditions corresponding to water saturation of the sponge): $0\text{--}350 \text{ mg Cs L}^{-1}$. The contact time before centrifugation and after water absorption can be as low as 1–2 min: this is sufficient to reach complete metal recovery under above-cited

experimental conditions. Preliminary tests on $^{137}\text{Cs(I)}$ recovery using the absorption/binding procedure confirm the high efficiency of the chitin-PB sponges for the treatment of radioelement dumped waters: the distribution coefficient reached up to $88,000 \text{ L g}^{-1}$.

The efficiency and competitiveness of sorption processes usually requires the desorption of the metal (for concentration effect and valorization) and the recycling of the sorbent for successive sorption/desorption cycles. This is especially necessary in the case of conventional base metals but this is less important in the case of noble metals (when cheap biosorbents are used the biomass can be burned or chemically degraded) or in the case of radionuclides. In the case of radioelements (such as our final target ^{137}Cs) the concentration effect may cause criticality problems and solid phases may be easier to manage for immobilizing and “inerting” the contaminated solid. For this reason cesium desorption was not investigated in this work. The present sorbent is stable in the wide range of pH at least in terms of encapsulating material (the reacetylation of chitosan improves chemical resistance of the biopolymer) and the stability of the sorbent for reuse is conditioned to the stability of the immobilized ion-exchanger. For conventional metals (which necessitate sorbent recycling) the desorption of the metal can be processed by acid elution or using a chelating agent.

References

- [1] P.J. Faustino, Y. Yang, J.J. Progar, C.R. Brownell, N. Sadrieh, J.C. May, E. Leutzinger, D.A. Place, E.P. Duffy, F. Houn, S.A. Loewke, V.J. Mecozzi, C.D. Ellison, M.A. Khan, A.S. Hussain, R.C. Lyon, Quantitative determination of cesium binding to ferric hexacyanoferrate: Prussian blue, *J. Pharm. Biomed. Anal.* 47 (2008) 114–125.
- [2] J. Ruprecht, Radiogardase® Prussian blue insoluble capsules, in: Heyl, Chemisch-Pharmazeutische, Fabrik GmbH Er Co., KG, Berlin, Germany, 2008.
- [3] S. Ayrault, C. Loos-Neskovic, M. Fedoroff, E. Garnier, Copper hexacyanoferrates – preparation, composition and structure, *Talanta* 41 (1994) 1435–1452.
- [4] P.A. Haas, A review of information on ferrocyanide solids for removal of cesium from solutions, *Sep. Sci. Technol.* 28 (1993) 2479–2506.
- [5] J. Lehto, S. Haukka, R. Harjula, M. Blomberg, Mechanism of cesium ion-exchange on potassium cobalt hexacyanoferrates(II), *J. Chem. Soc. Dalton Trans.* (3) (1990) 1007–1011.
- [6] T. Vincent, C. Vincent, Y. Barré, Y. Guari, G. Le Saout, E. Guibal, Immobilization of metal hexacyanoferrate in chitin beads for cesium sorption: synthesis and characterization, *J. Mater. Chem. A* 2 (2014) 10007–10021.
- [7] T. Yasutaka, T. Kawamoto, Y. Kawabe, T. Sato, M. Sato, Y. Suzuki, K. Nakamura, T. Komai, Rapid measurement of radiocesium in water using a Prussian blue impregnated nonwoven fabric: Fukushima NPP accident related, *J. Nucl. Sci. Technol.* 50 (2013) 674–681.
- [8] A.K. Vipin, B. Hu, B. Fugetsu, Prussian blue caged in alginate/calcium beads as adsorbents for removal of cesium ions from contaminated water, *J. Hazard. Mater.* 258 (2013) 93–101.
- [9] A. Kitajima, H. Tanaka, N. Minami, K. Yoshino, T. Kawamoto, Efficient cesium adsorbent using Prussian blue nanoparticles immobilized on cotton matrices, *Chem. Lett.* 41 (2012) 1473–1474.
- [10] B. Hu, B. Fugetsu, H. Yu, Y. Abe, Prussian blue caged in spongiform adsorbents using diatomite and carbon nanotubes for elimination of cesium, *J. Hazard. Mater.* 217–218 (2012) 85–91.

- [11] C. Dwivedi, A. Kumar, K.K. Singh, A.K. Juby, M. Kumar, P.K. Wittal, P.N. Bajaj, Copper hexacyanoferrate-polymer composite beads for cesium ion removal: synthesis, characterization, sorption, and kinetic studies, *J. Appl. Polym. Sci.* 129 (2013) 152–160.
- [12] Z. Du, M. Jia, X. Wang, Cesium removal from solution using PAN-based potassium nickel hexacyanoferrate (II) composite spheres, *J. Radioanal. Nucl. Chem.* 298 (2013) 167–177.
- [13] V. Avramenko, S. Bratskaya, V. Zheleznov, I. Sheveleva, D. Marinin, V. Sergienko, Asme, Latex particles functionalized with transition metals ferrocyanides for cesium uptake and decontamination of solid bulk materials, ASME, *Env Engn; ASME, Nucl Engn Div Tsukuba, Japan*, (2011).
- [14] H. Mimura, Y. Onodera, Selective uptake and recovery of cesium ions by composite columns of ammonium molybdophosphate (AMP)-calcium alginate, *J. Nucl. Sci. Technol.* 39 (2002) 282–285.
- [15] P. Krys, F. Testa, A. Trochimczuck, C. Pin, J.M. Taulemesse, T. Vincent, E. Guibal, Encapsulation of ammonium molybdophosphate and zirconium phosphate in alginate matrix for the sorption of Rb(1), *J. Colloid Interface Sci.* 409 (2013) 141–150.
- [16] A. Tokarev, P. Agulhon, J. Long, F. Quignard, M. Robitzer, R.A.S. Ferreira, L.D. Carlos, J. Larionova, C. Guerin, Y. Guari, Synthesis and study of Prussian blue type nanoparticles in an alginate matrix, *J. Mater. Chem.* 22 (2012) 20232–20242.
- [17] B. Folch, J. Larionova, Y. Guari, K. Molvinger, C. Luna, C. Sangregorio, C. Innocenti, A. Caneschi, C. Guerin, Synthesis and studies of water-soluble Prussian blue-type nanoparticles into chitosan beads, *Phys. Chem. Chem. Phys.* 12 (2010) 12760–12770.
- [18] C.K.S. Pillai, W. Paul, C.P. Sharma, Chitin and chitosan polymers: chemistry, solubility and fiber formation, *Progr. Polym. Sci.* 34 (2009) 641–678.
- [19] T. Vincent, E. Guibal, Cr(VI) extraction using aliquat 336 in a hollow fiber module made of chitosan, *Ind. Eng. Chem. Res.* 40 (2001) 1406–1411.
- [20] S.V. Madihally, H.W.T. Matthew, Porous chitosan scaffolds for tissue engineering, *Biomaterials* 20 (1999) 1133–1142.
- [21] W.-C. Hsieh, C.-P. Chang, S.-M. Lin, Morphology and characterization of 3D micro-porous structured chitosan scaffolds for tissue engineering, *Colloid Surf. B* 57 (2007) 250–255.
- [22] T. Andersen, J.E. Melvik, O. Gasered, E. Alsberg, B.E. Christensen, Ionically gelled alginate foams: physical properties controlled by operational and macromolecular parameters, *Biomacromolecules* 13 (2012) 3703–3710.
- [23] M. Lavertu, V. Darraas, M.D. Buschmann, Kinetics and efficiency of chitosan reacylation, *Carbohydr. Polym.* 87 (2012) 1192–1198.
- [24] P. Sorlier, A. Denuziere, C. Viton, A. Domard, Relation between the degree of acetylation and the electrostatic properties of chitin and chitosan, *Biomacromolecules* 2 (2001) 765–772.
- [25] E. Guibal, S. Cambe, S. Bayle, J.-M. Taulemesse, T. Vincent, Silver/chitosan/cellulose fibers foam composites: from synthesis to antibacterial properties, *J. Colloid Interface Sci.* 393 (2013) 411–420.
- [26] C. Jouannin, C. Vincent, I. Dez, A.-C. Gaumont, T. Vincent, E. Guibal, Study of alginate-supported ionic liquid and Pd catalysts, *Nanomaterials* 2 (2012) 31–53.
- [27] N.-Y. Yuan, Y.-A. Lin, M.-H. Ho, D.-M. Wang, J.-Y. Lai, H.-J. Hsieh, Effects of the cooling mode on the structure and strength of porous scaffolds made of chitosan, alginate, and carboxymethyl cellulose by the freeze-gelation method, *Carbohydr. Polym.* 78 (2009) 349–356.
- [28] D.W. Ren, H.F. Yi, W. Wang, X.J. Ma, The enzymatic degradation and swelling properties of chitosan matrices with different degrees of N-acetylation, *Carbohydr. Res.* 340 (2005) 2403–2410.
- [29] C. Suwanchawalit, A.J. Patil, R.K. Kumar, S. Wongnawa, S. Mann, Fabrication of ice-templated macroporous TiO₂-chitosan scaffolds for photocatalytic applications, *J. Mater. Chem.* 19 (2009) 8478–8483.